Open Access Library Journal
2017, Volume 4, e4237
ISSN Online: 2333-9721
ISSN Print: 2333-9705

Research on Permanent Magnet Synchronous Motor Driver System of Horizontal Well Tractor

Zhou He, Yongjun Chen*, Shuhan Yu, Junwen Zhou, Yang Shen, Kuan Shi

College of Electronics and Information, Yangtze University, Jingzhou, China
Email: *952481907@qq.com

How to cite this paper: He, Z., Chen, Y.J., Yu, S.H., Zhou, J.W., Shen, Y. and Shi, K. (2017) Research on Permanent Magnet Synchronous Motor Driver System of Horizontal Well Tractor. *Open Access Library Journal*, **4**: e4237.
https://doi.org/10.4236/oalib.1104237

Received: December 5, 2017
Accepted: December 25, 2017
Published: December 28, 2017

Abstract

Nowadays, horizontal well technology is being applied to the development of oilfield production capacity more and more. The horizontal well tractor can effectively solve the problem that the instrument can not get to the target layer by gravity. However, in actual conditions, Brushless DC motor (BLDCM) there is a large torque ripple problem, resulting in motor running is not smooth, vibration and noise is too large, can not meet the demand. Therefore, propose horizontal well tractor PMSM sine wave drive technology. The paper discusses the mathematical model of permanent magnet synchronous motor, analyzes the working principle of space vector pulse width modulation (SVPWM) technology, and establishes a speed and current double closed-loop space vector control system of the permanent magnet synchronous motor by using PSIM simulation software. Simulation results verify the robustness of the control system, and the torque ripple of the motor is small, in line with the working conditions of horizontal well tractor.

Subject Areas

Electric Engineering

Keywords

Horizontal Well Tractor, PSIM, Permanent Magnet Synchronous Motor (PMSM), Space Vector Pulse Width Modulation (SVPWM)

1. Introduction

Horizontal well technology is increasingly being applied to the development of oilfield productivity. Today, the horizontal well tractor is a transport tool for logging tools in horizontal well logging technology, which solves the problem that the instrument can't get to the target layer by gravity. The brushless DC motor

(BLDCM) used for horizontal well tractor has large torque ripple in the actual condition, the motor running not smooth, vibration and noise is too large, can not meet the demand. In view of the above reasons, this paper proposes a permanent magnet synchronous motor (PMSM) of horizontal well tractor sine wave drive technology through the research of control algorithm, to improve the dynamic performance of the system [1] [2].

Based on the analysis of the mathematical model of PMSM and its vector control principle and the Space Vector Pulse Width Modulation (SVPWM) algorithm [3] [4], a PMSM control system based on SVPWM control algorithm is established by using PSIM (Power Simulation), which realizes the speed and current double closed loop space vector control system of PMSM. The simulation results and analysis are given [5] [6]. The results show that the system has good robustness and the torque ripple of the motor is small, and meets the demand of horizontal well tractors.

2. Mathematical Model of PMSM and Its Vector Control Principle

The mathematical model of PMSM in the synchronous rotating coordinate system as follows [7]:

Motor flux linkage equation:

$$\begin{cases} \psi_d = L_d i_d + \psi_f \\ \psi_q = L_q i_q \end{cases} \tag{1}$$

Stator voltage equation:

$$\begin{cases} u_d = R_s i_d + \dfrac{\mathrm{d}\psi_d}{\mathrm{d}t} - \omega_e \psi_q \\ u_q = R_s i_q + \dfrac{\mathrm{d}\psi_q}{\mathrm{d}t} + \omega_e \psi_d \end{cases} \tag{2}$$

Torque equation:

$$T_e = \frac{3}{2} p_n \left(\psi_d i_q - \psi_q i_d \right) \tag{3}$$

Equation of motion:

$$T_e - T_L = J \frac{\mathrm{d}\omega}{\mathrm{d}t} + B\omega \tag{4}$$

In type: ψ_d, ψ_q is the flux linkage of d, q axis; L_d, L_q is inductance of d, q axis; i_d, i_q is current of d, q axis; ψ_f is flux linkage of permanent; R_s is resistance of stator; ω_e, ω is the electrical angular speed and mechanical angular speed of the rotor; T_e is electromagnetic torque; p_n is the number of pole pairs of a motor; T_L is Load torquer; J is moment of inertia; B is friction factor.

According to Equations (1)-(3), if $i_d = 0$ can be obtained:

$$T_e = \frac{3}{2} p_n \psi_f i_q \tag{5}$$

From the above, it can be found that the electromagnetic torque of the motor is determined only by the current of *q*-axis, which realizes the decoupling of electromagnetic torque of the motor. Thus, It can be seen that after adopting the $i_d = 0$ control mode, the permanent magnet synchronous motor is equivalent to a self excitation DC motor, which only needs to control the torque current i_q, and can control the electromagnetic torque, so as to achieve speed control. Figure 1 is the schematic diagram of PMSM Vector Control:

3. Principle of SVPWM Algorithm

SVPWM refers to the different combinations of the switching tubes of the bridge arm of the three-phase inverter bridge and outputs different pulse sequences for controlling the inverter to output three-phase sinusoidal voltage or three-phase sinusoidal current. Figure 2 is a schematic diagram of three phase inverter:

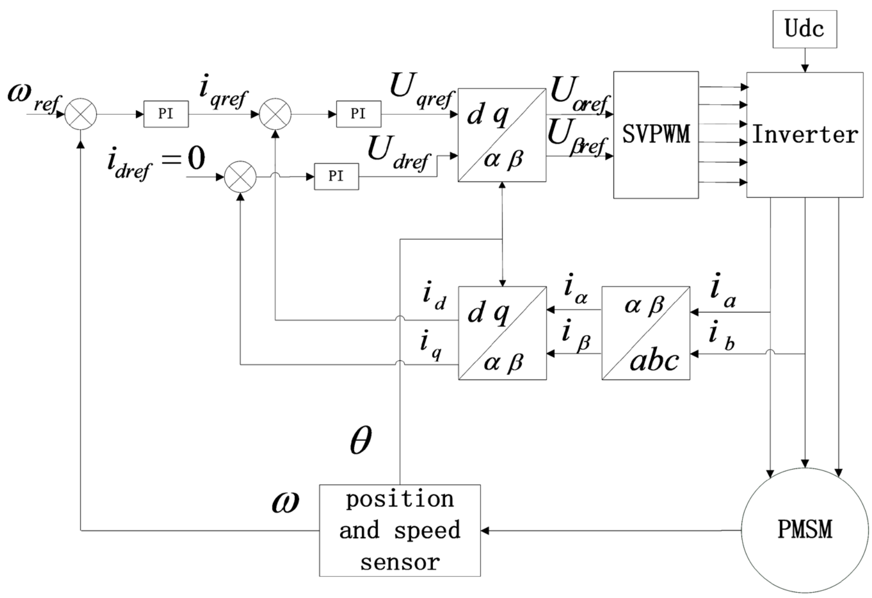

Figure 1. Schematic diagram of PMSM vector control.

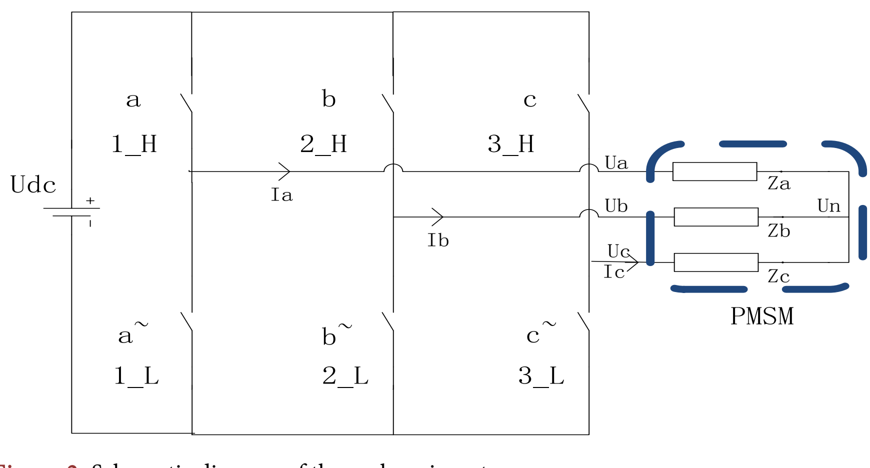

Figure 2. Schematic diagram of three phase inverter.

It can be seen from the schematic diagram of the three-phase inverter that six switching devices are controlled by six control signals. Each of the upper and lower bridge switching devices can only be turned on and the other one is turned off. Therefore, the inverter has 8 operating states. Corresponding to 8 voltage vectors. Set on the bridge conduction, the lower bridge off as 1, the lower bridge conduction, the bridge off recorded as zero. The formula for the phase voltage can be derived:

$$\begin{bmatrix} u_a \\ u_b \\ u_c \end{bmatrix} = \frac{1}{3} U_{dc} \begin{bmatrix} 2 & -1 & -1 \\ -1 & 2 & -1 \\ -1 & -1 & 2 \end{bmatrix} \begin{bmatrix} a \\ b \\ c \end{bmatrix} \tag{6}$$

u_a, u_b, u_c indicates the three-phase stator voltage in $a-b-c$ coordinate system, the u_α, u_β in the $\alpha-\beta$ coordinate system can be got by using the clark transformation:

$$\begin{bmatrix} u_\alpha \\ u_\beta \end{bmatrix} = \sqrt{\frac{2}{3}} \begin{bmatrix} 1 & -\frac{1}{2} & -\frac{1}{2} \\ 0 & \frac{\sqrt{3}}{2} & -\frac{\sqrt{3}}{2} \end{bmatrix} \begin{bmatrix} u_a \\ u_b \\ u_c \end{bmatrix} \tag{7}$$

Distributions of 8 voltage vector $U_1 \sim U_6, O_{000}, O_{111}$ such as **Figure 3**:

From **Figure 3**, it can be seen that 2 of the 8 basic space voltage vectors are zero vectors, the other 6 non zero vector amplitudes are equal, and the phase difference is 60 degrees, dividing vector space into 6 sectors. According to the parallelogram rule, the 8 basic space vectors can be used to synthesize any voltage vector. SVPWM that does not exceed the maximum amplitude. SVPWM technology is to use these 8 basic spatial vectors to approximate the given reference voltage vectors U_{ref}. In order to meet the requirement of the actual working condition of the horizontal well tractor, the actual flux linkage vector is made to approximate the ideal circle track of the flux linkage and reduce the torque ripple of the motor.

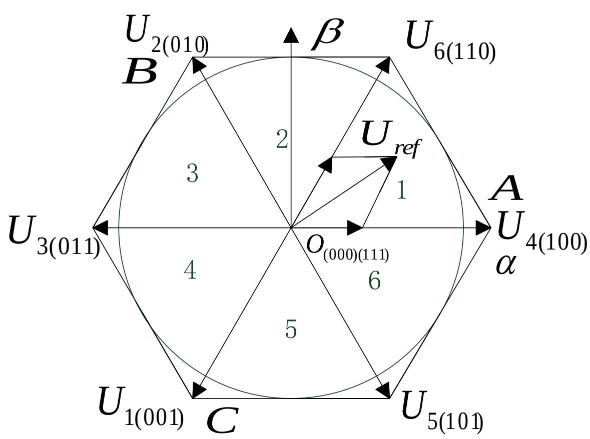

Figure 3. Basic space vector distribution map.

4. Implementation of SVPWM Algorithm

4.1. Determine the Sector of the U_{ref}

Set up 3 reference quantities:

$$\begin{cases} U_{ref1} = u_\beta \\ U_{ref2} = \frac{1}{2}\left(\sqrt{3}u_\alpha - u_\beta\right) \\ U_{ref3} = -\frac{1}{2}\left(\sqrt{3}u_\alpha + u_\beta\right) \end{cases} \tag{8}$$

It can be seen from Figure 3, If $U_{ref1} = 0$, $U_{ref2} = 0$, $U_{ref3} = 0$, 3 lines can be got that reclosing with 6 non zero vectors, thus, According to the relation between 3 reference quantities and the size of 0, the sector of U_{ref} can be determined. Setting up 4 auxiliary variables N, x, y, z, if $U_{ref1} > 0$, $x = 1$, otherwise $x = 0$; if $U_{ref2} > 0$, $y = 1$, otherwise, $y = 0$; if $U_{ref3} > 0$, $z = 1$, otherwise, $z = 0$:

$$N = x + 2y + 4z \tag{9}$$

relation between N and sector following Table 1.

4.2. Determine the Time of Action of Adjacent Vectors T_1, T_2

It can be known that U_{ref} is synthesized by two vectors in its sector through principle of SVPWM algorithm. As shown in Figure 3. U_{ref} in the 1 sector, formula is as follows:

$$\begin{cases} TU_{ref} = T_1U_4 + T_2U_6 + T_0O_{000\,(111)} \\ T = T_1 + T_2 + T_0 \end{cases} \tag{10}$$

In type: T is period of PWM; T_1, T_2, T_0 is time of action of U_4, U_6 and $O_{000(111)}$.

Equation can be obtained by converting reference voltage vector to $\alpha-\beta$ coordinate system:

$$\begin{cases} U_{\alpha ref} = \frac{T_1}{T}\left|U_4\right| + \frac{T_2}{T}\left|U_6\right|\cos\frac{\pi}{3} \\ U_{\beta ref} = \frac{T_2}{T}\left|U_6\right|\sin\frac{\pi}{3} \end{cases} \tag{11}$$

Because of $\left|U_4\right| = \left|U_6\right| = \frac{2}{3}U_{dc}$, Equation can be obtained:

$$\begin{cases} T_1 = \frac{1}{2}\left(\sqrt{3}U_{\alpha ref} - U_{\beta ref}\right)\frac{\sqrt{3}T}{U_{dc}} = \frac{\sqrt{3}T}{U_{dc}}U_{ref2} \\ T_2 = U_{\beta ref}\frac{\sqrt{3}T}{U_{dc}} = \frac{\sqrt{3}T}{U_{dc}}U_{ref1} \end{cases} \tag{12}$$

$T_x = \frac{\sqrt{3}T}{U_{dc}}U_x$ can be seen from the form (12). For different sectors, relation between U_1, U_2 and $U_{ref1}, U_{ref2}, U_{ref3}$ following Table 2.

Table 1. Table of relation between N and sector.

N	1	2	3	4	5	6
sector	2	6	1	4	3	5

Table 2. Table of relation between U_1, U_2 and $U_{ref1}, U_{ref2}, U_{ref3}$.

N	3	1	5	4	6	2
U_1	U_{ref2}	$-U_{ref2}$	U_{ref1}	$-U_{ref1}$	U_{ref3}	$-U_{ref3}$
U_2	U_{ref1}	$-U_{ref3}$	U_{ref3}	$-U_{ref2}$	U_{ref2}	$-U_{ref1}$

4.3. Determine the SVPWM Waveform

The SVPWM waveform used in this paper uses a more widely used seven stage synthesis method. Take 1 sectors as an example, in order to divide the action time of each vector into two parts, and divide the time of zero vector action to two zero vectors, we can minimize the number of switches per bridge and effectively reduce the output harmonic content of the inverter. The synthesized vector sequence is like Table 3, and the generated SVPWM waveform is following Figure 4.

The corresponding comparison values t_a, t_b, t_c can be obtained from Figure 4:

$$\begin{cases} t_a = \dfrac{(T - T_1 - T_2)}{4T} \\ t_b = t_a + \dfrac{T_1}{2T} = \dfrac{(T + T_1 - T_2)}{4T} \\ t_c = t_b + \dfrac{T_2}{2T} = \dfrac{(T + T_1 + T_2)}{4T} \end{cases} \tag{13}$$

The relationship between the comparison value and t_a, t_b, t_c in different sectors is following Table 4. It can be known from Figure 4 that the corresponding SVPWM waveform can be obtained after comparing the obtained comparison value with the triangular wave.

4.4. Implementation of SVPWM Algorithm in PSIM

PSIM is a computer simulation software dedicated to the design and analysis of power electronic circuits and motor control systems. PSIM has a simplified C block, and users can implement a control algorithm by writing a C language program. The following details are introduced by using PSIM software to implement the SVPWM algorithm through the simplified C Block.

As in Figure 5, the above module uses a total of 4 block. Block 1 calculate $U_{ref1}, U_{ref2}, U_{ref3}$ based on U_α, U_β, block 2 calculate N based on $U_{ref1}, U_{ref2}, U_{ref3}$, block 3 calculate t_a, t_b, t_c based on $U_{ref1}, U_{ref2}, U_{ref3}$, N and the bus voltage obtained through a voltage sensor, block 4 get the corresponding comparison value signal based on t_a, t_b, t_c and N. Then through the comparison

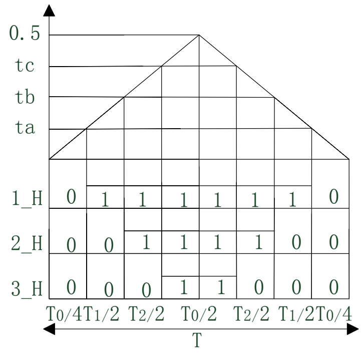

Figure 4. SVPWM waveform.

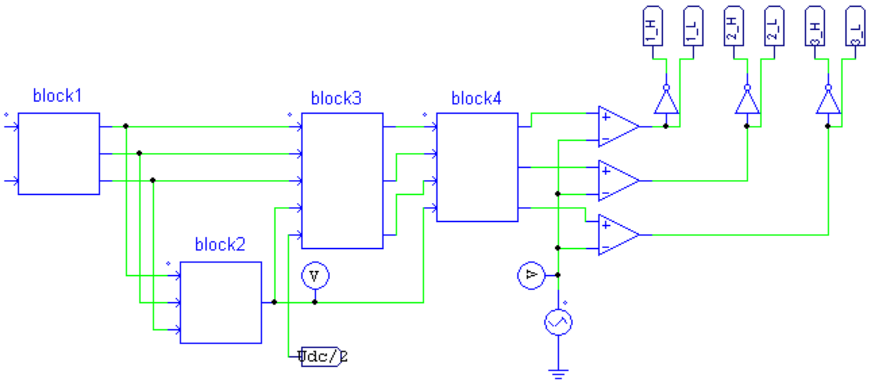

Figure 5. SVPWM algorithm module.

Table 3. Vector sequence table.

$\frac{T_0}{4}$	$\frac{T_1}{2}$	$\frac{T_2}{2}$	$\frac{T_0}{2}$	$\frac{T_2}{2}$	$\frac{T_1}{2}$	$\frac{T_0}{4}$
O_{000}	U_{100}	U_{110}	O_{111}	U_{110}	U_{100}	O_{000}

Table 4. Table of relations between comparison values and t_a, t_b, t_c.

N	3	1	5	4	6	2
T_{cm1}	t_a	t_b	t_c	t_c	t_b	t_a
T_{cm2}	t_b	t_a	t_a	t_b	t_c	t_c
T_{cm3}	t_c	t_c	t_b	t_a	t_a	t_b

with the triangular wave to form SVPWM signal to control the inverter, in order to achieve SVPWM algorithm.

5. Establishment of PMSM Control System

The PMSM control system following **Figure 6** is constructed by using the SVPWM algorithm module and the PSIM model library constructed as described above. There are various simulation models of motor and power

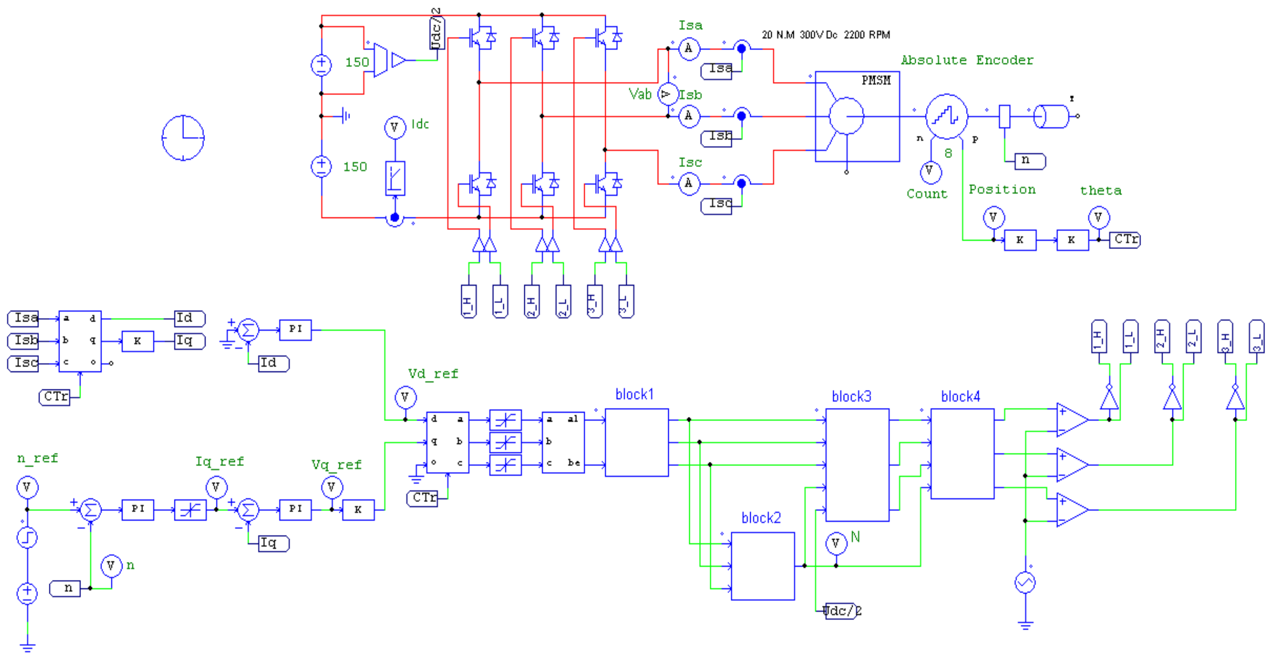

Figure 6. PMSM control system.

Table 5. PMSM simulation parameters.

DC bus voltage/V	rated torque/N·m	rated speed/rpm	number of pole pairs	back EMF constant /V·krpm^{-1}
300	20	2200	4	25.9192
stator resistance/Ω	Stator d-axis inductor/mH	Stator q-axis inductance/mH	moment of inertia/kg·m^2	friction factor/kg·m^2·s^{-1}
0.129	1.453	1.607	3.334×10^{-3}	4.25×10^{-4}

electronic devices in the model reservoir of PSIM, which can facilitate the user to establish the control system.

Shown in **Figure 6**, the three-phase inverter switching devices using IGBT, PMSM simulation parameters in **Table 5**, the control system uses speed, current double closed-loop PI control, which obtains the output of the electrical angle and speed by absolute encoder and speed sensor.

6. Simulation Results and Analysis

The control system in this paper: The given DC bus voltage is 300 V. Period of PWM is 50 μs. The motor load torque is 20 N·m. The simulation time is 0.4 s. The initial given speed of motor is 1700 rpm. At 0.2 s, the given speed changes from 1700 to 2200 rpm. The simulation results are shown in **Figures 7-12**. It can be seen that the stator three-phase current is very close to the standard sine wave, the speed and torque dynamic response fast, the system quickly into the steady state, closed-loop PI control plays a good role, the motor torque ripple is small, in line with the horizontal well tractor The actual conditions of demand.

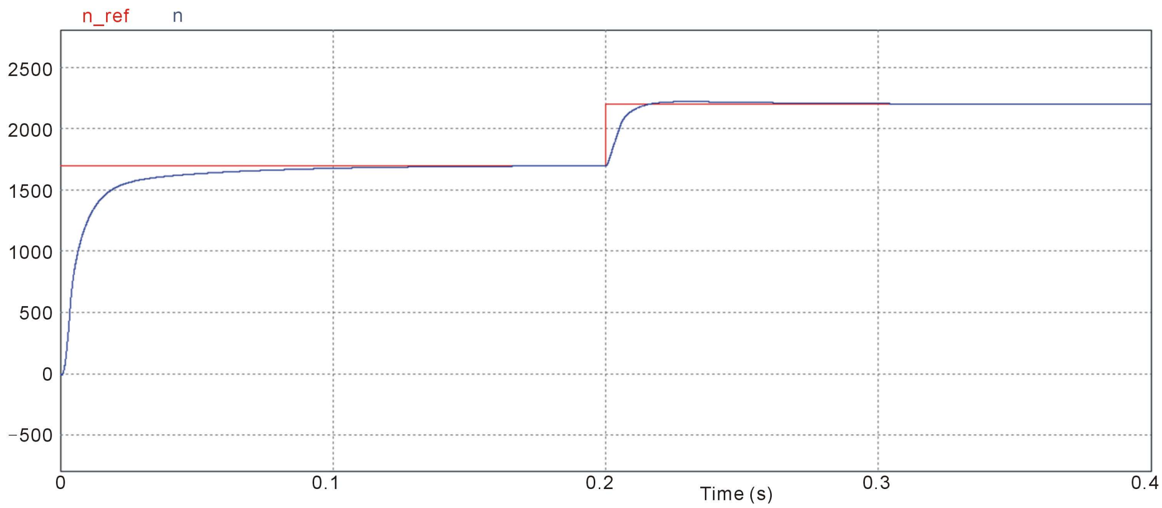

Figure 7. Speed waveform diagram.

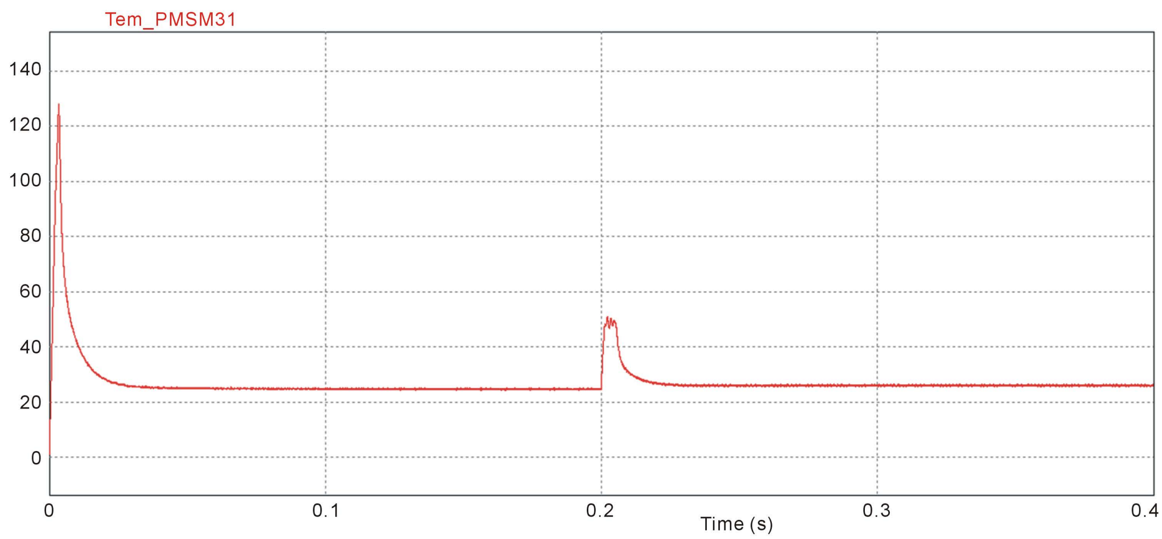

Figure 8. Torque waveform.

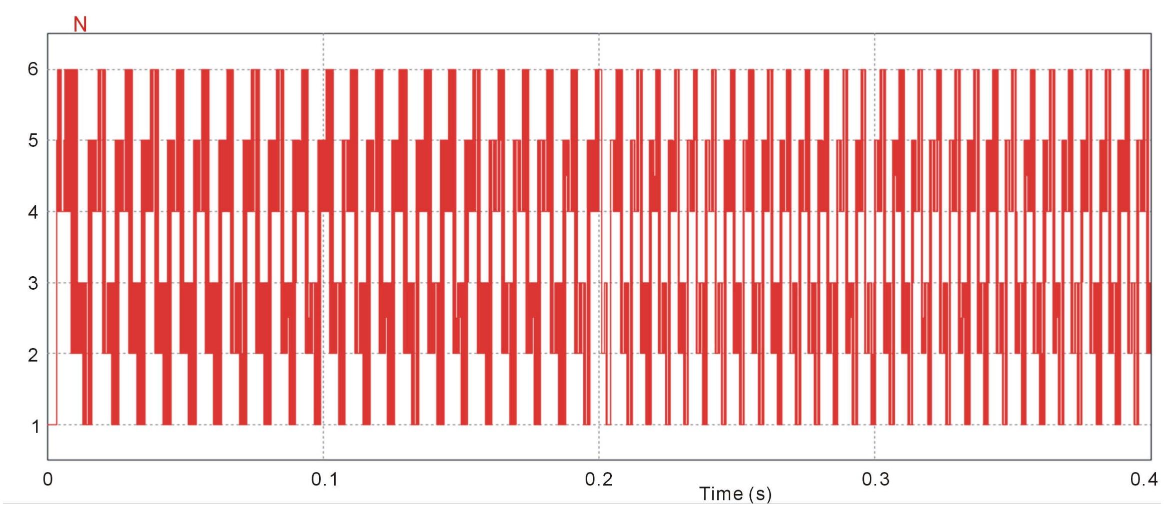

Figure 9. Sector change diagram of U_{ref}.

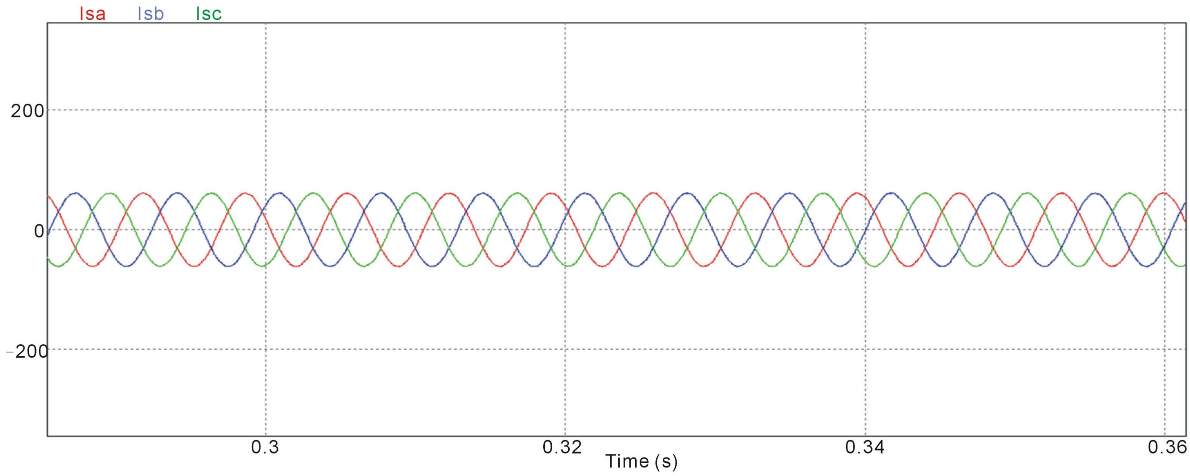

Figure 10. Stator three-phase current waveform.

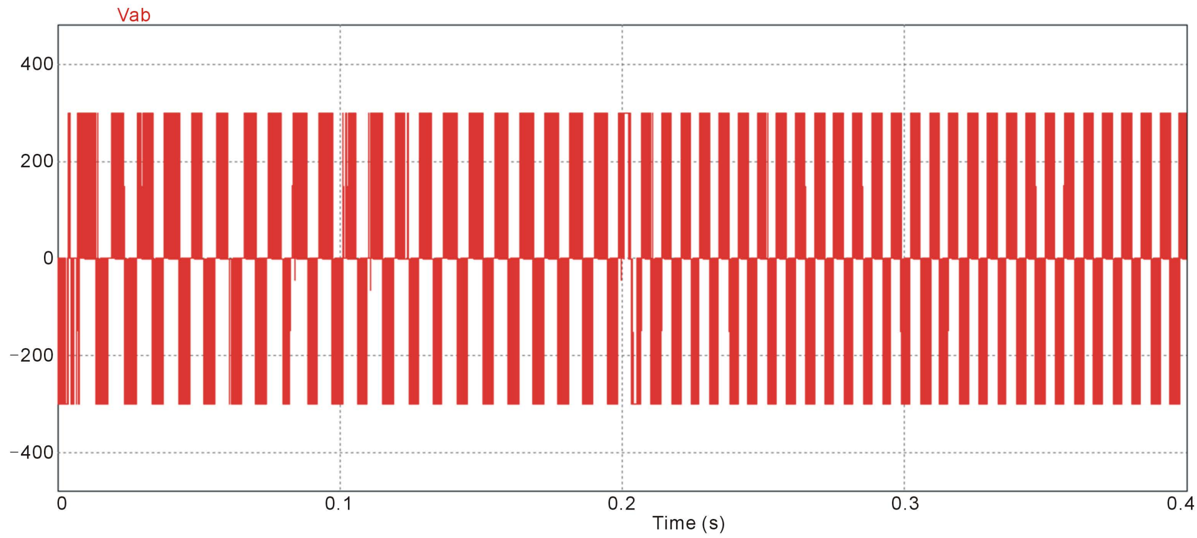

Figure 11. Line voltage waveform.

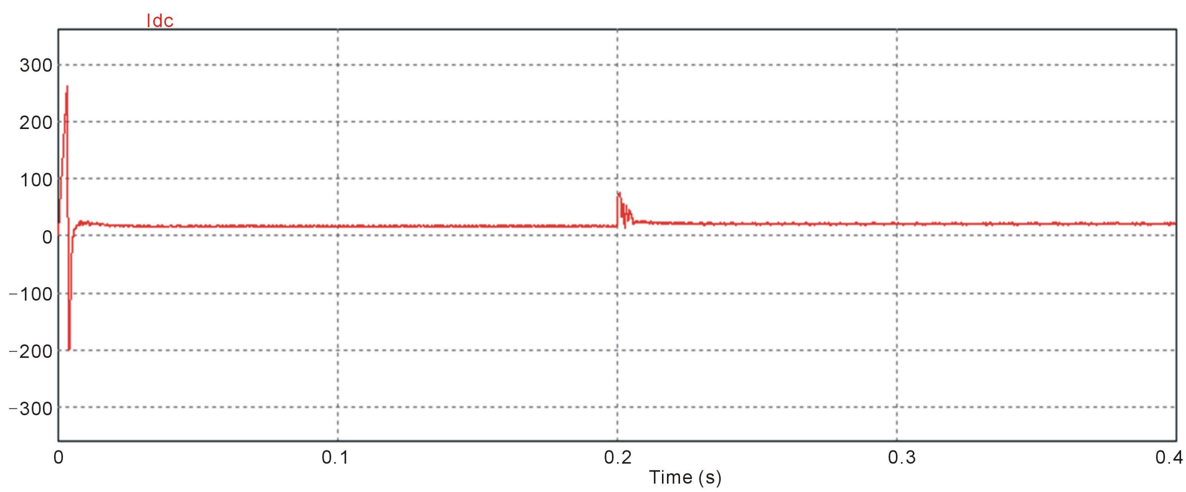

Figure 12. DC bus current.

7. Conclusion

The simulation circuit of PMSM control system based on SVPWM algorithm is established by using PSIM software and the PMSM closed-loop vector control system with control mode is realized. The simulation results show that the control system has strong robustness, small torque ripple, in line with the working conditions of horizontal well tractor.

Foundation Project

The subject of the research association of the work of Hubei college laboratory in 2016, project number HBSY2016-25; the research project of colleges and universities' provincial teaching in Hubei in 2016, project number 2016-258.

References

[1] Scarcella, G., Scelba, G., Pulvirenti, M., *et al.* (2017) Fault-Tolerant Capability of Deadbeat-Direct Torque and Flux Control for Three-Phase PMSM Drives. *IEEE Transactions on Industry Applications*, **53**, 5496-5508. https://doi.org/10.1109/TIA.2017.2743070

[2] Formentini, A., Trentin, A., Marchesoni, M., *et al.* (2015) Speed Finite Control Set Model Predictive Control of a PMSM Fed by Matrix Converter. *IEEE Transactions on Industrial Electronics*, **62**, 6786-6796. https://doi.org/10.1109/TIE.2015.2442526

[3] Kontarček, A., Bajec, P., Nemec, M., *et al.* (2015) Cost-Effective Three-Phase PMSM Drive Tolerant to Open-Phase Fault. *IEEE Transactions on Industrial Electronics*, **62**, 6708-6718. https://doi.org/10.1109/TIE.2015.2437357

[4] Preindl, M. and Bolognani, S. (2013) Model Predictive Direct Torque Control with Finite Control Set for PMSM Drive Systems, Part 1: Maximum Torque per Ampere Operation. *IEEE Transactions on Industrial Informatics*, **9**, 1912-1921. https://doi.org/10.1109/TII.2012.2227265

[5] Inoue, Y., Morimoto, S. and Sanada, M. (2012) Comparative Study of PMSM Drive Systems Based on Current Control and Direct Torque Control in Flux-Weakening Control Region. *IEEE Transactions on Industry Applications*, **48**, 2382-2389. https://doi.org/10.1109/TIA.2012.2227134

[6] Hu, J.H., Zou, J.B., Xu, F., Li, Y., *et al.* (2012) An Improved PMSM Rotor Position Sensor Based on Linear Hall Sensors. *IEEE Transactions on Magnetics*, **48**, 3591-3594. https://doi.org/10.1109/TMAG.2012.2202279

[7] Zou, J.B., Zhao, B., Xu, Y.X., *et al.* (2012) A New End Windings Transposition to Reduce Windings Eddy Loss for 2 MW Direct Drive Multi-Unit PMSM. *IEEE Transactions on Magnetics*, **48**, 3323-3326. https://doi.org/10.1109/TMAG.2012.2201701